

# Two-dimensional Analytical Modelling of a Direct Methanol Fuel Cell

P. Alotto, M. Guarnieri and F. Moro

Dipartimento di Ingegneria Elettrica  
Università di Padova

Via Gradenigo, 6/A, 35131 Padova (Italy)

Phone number: +0039 049 8277567, e-mail: [alotto@die.unipd.it](mailto:alotto@die.unipd.it)

Phone number: +0039 049 8277524, e-mail: [guarnieri@die.unipd.it](mailto:guarnieri@die.unipd.it)

Phone number: +0039 049 8277550, e-mail: [moro@die.unipd.it](mailto:moro@die.unipd.it)

**Abstract.** Direct methanol fuel cells are regarded nowadays as promising energy sources for portable electronic devices. Numerical models can be very useful for addressing the exploration of the fuel cell performance, without the development of many prototypes, which can be very expensive due to the presence of rare materials. Analytical models are particularly suited for investigating the cell performance with limited computing costs.

In this work, a two-dimensional model for assessing the performance of an active-feed direct methanol fuel cell is presented, accounting for electrochemical reactions, mass and heat transfer.

## Key words

Fuel cell, methanol, DMFC, renewable energy, multi-physics, mathematical model.

## 1. Introduction

Among the different technological solutions for fuel cells presently developed, Direct Methanol Fuel Cells (DMFCs) are a promising kind of electrical generators, subject to research and development activities in many laboratories around the world. Operating at low temperatures, they appear suitable to provide power for portable devices in the next future and, further away, to supply power to electrical motors in automotive applications.

In DMFCs, which are now working at near room temperature, the fuel is a water-methanol solution directly fed at the anode without any hydrogen reforming procedure, while the cathode is fed with air. Methanol is much easier and safe to handle than hydrogen, thus avoiding safety measures needed with the latter. DMFCs consist of a proton-conducting polymeric membrane (PEM) and two electro-catalysts based on noble metals (mostly platinum and ruthenium). These features lead to a cell structure which is very compact, simple and lightweight, with passive fuel feed and suitable for miniaturization.

The development of DMFCs typically follows two research paths: the first one centred on the synthesis of new materials for PEMs and electro-catalysts; the second one related to the production of multi-physics analytical and numerical models, able to simulate the overall cell behaviour in order to simulate experimental set-ups and to provide tools for the development of industrial optimized designs of minimum size. A multi-sector research group is working at Padova University on both of these lines. The chemical research is focused on improving the performance of cell materials and assemblies, while engineering activities are concerned with the development of mathematical models [2][3].

In this work a two-dimensional model, has been implemented in order to perform feed-forward analyses of various cell configurations and design optimizations. The analytical model of the DMFC accounts for the following phenomena:

- electrochemical reactions occurring at catalyst layers;
- protonic conduction and methanol crossover across the PEM;
- diffusion of reactants in porous media layers;
- fluid motion inside flow channels;
- coupled heat and mass transfer.

The fuel cell model presented here is based on the two-dimensional and one-dimensional models proposed in [4][5].

A schematic representation of a single fuel cell inside a stack is sketched in Fig. 1. It consists basically of an anode flow channel (AFC), an anode diffusion layer (ADL), an anode catalyst layer (ACL), a proton exchange membrane (PEM), a cathode catalyst layer (CCL), a cathode diffusion layer (CDL) and a cathode flow channel (CFC). The model is two-dimensional in the sense that varying methanol/oxygen concentrations inside anode/cathode flow channels (along y-axis of Fig. 1) are taken into account. Conversely, the modelled phenomena inside the fuel cell such as mass/heat transfer and diffusion are directed mainly along the x-axis.

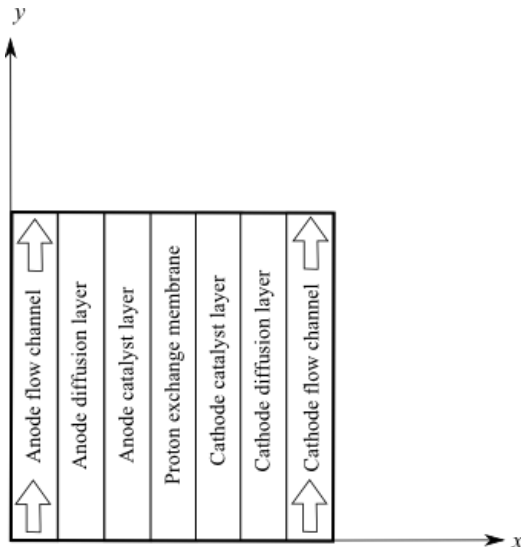


Fig. 1. Schematic view of an active-feed DMFC.

## 2. Direct Methanol Fuel Cell Model

### A. Basic assumptions of the fuel cell model

The following approximations, concerning the physical behaviour of each section of the fuel cell, are considered:

- Water at cathode is at the vapour state (single-phase assumption);
- The air at the cathode flow channel is in a saturated state;
- The air temperature on the cathode flow channel is constant;
- Catalyst layers are at constant temperature, since they are much thinner than gas diffusion layers;
- Transport of reactants along the y-axis in catalyst and diffusion layers is neglected as their thickness are two orders of magnitude less than their widths;
- The concentration change of reactants across catalyst layers (x-axis) is neglected as the thickness of diffusion layers is one order of magnitude larger than that of catalyst layers;
- The variation of the overpotential across catalyst layers and along the y-axis is small;
- As regards temperature computation, Joule power losses on the membrane are neglected with respect to reaction and overpotential heat;
- The crossover methanol completely reacts at the cathode catalyst layer, so the methanol concentration is negligible there;
- Methanol crossover through the membrane is due to a combined effect between diffusion, i.e. the concentration gradient, and electro-osmosis.

### B. Physical quantities in the fuel cell model

For the sake of clarity, the main physical variables used for modelling the DMFC are listed in the table below.

In the following, subscripts *ah*, *ad*, *ac* indicate variables related to the anode flow channel, anode gas diffusion

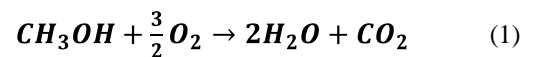
layer, and anode catalyst layer, respectively; *ch*, *cd*, *cc* similarly refer to the cathode side subscript; finally, *m* indicates the membrane.

TABLE I. – Main variables and constants of the DMFC model.

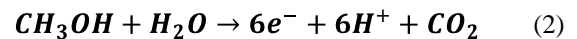
Parameter	Symbol	Unit
Fuel cell voltage	$V$	V
Electric current density	$J$	$A \cdot m^{-2}$
Fuel cell std. potential	$E$	V
Activation overpotential	$\eta$	V
Molar concentration	$C$	$mol \cdot m^{-3} / M$
Molar flow	$N$	$mol \cdot s^{-1}$
Temperature	$T$	K
Specific heat flow	$q$	$W \cdot m^{-2}$
Fluid velocity	$v$	$m \cdot s^{-1}$
Dimensionless parameter	$\xi$	
Diffusion coefficient	$D$	$m^2 \cdot s^{-1}$
Electro-osmotic drag coeff.	$n_d$	-
Volume flow rate	$m$	$m^3 \cdot s^{-1}$
Transfer coefficient	$a$	-
Number of flow channels	$n_{ch}$	-
Depth/thickness	$\delta$	m
Width	$w$	m
Length	$l$	m
Proton conductivity	$\sigma$	$S \cdot m^{-1}$
Horizontal coordinate	$x$	m
Vertical coordinate	$y$	m
Universal gas constant	$R$	$J \cdot mol^{-1} \cdot K^{-1}$
Faraday constant	$F$	$A \cdot s \cdot mol^{-1}$
Temperature in std. conditions	$T_o$	K

### C. Analytical solution of the cell voltage

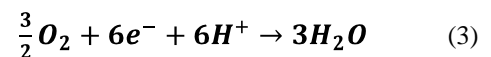
The complete anode/cathode reaction of methanol oxidation in DMFC:



is split into two main partial reactions by effect of the proton exchange membrane (PEM) as:



at the anode catalyst layer, and



at the cathode catalyst layer. (2) and (3) state that methanol is oxidized at the anode catalyst layer, while both oxygen reduction and crossover methanol oxidation occur at the anode. According to (2), a consumption of 1 mol of methanol can generate 6 mol of electrons. These electrons flow through the external electrical circuit and close their path at the cathode, providing the electric power of the electrochemical generator.

A diagram explaining reactant and particle flows inside a typical direct methanol fuel cell is provided in Fig. 2.

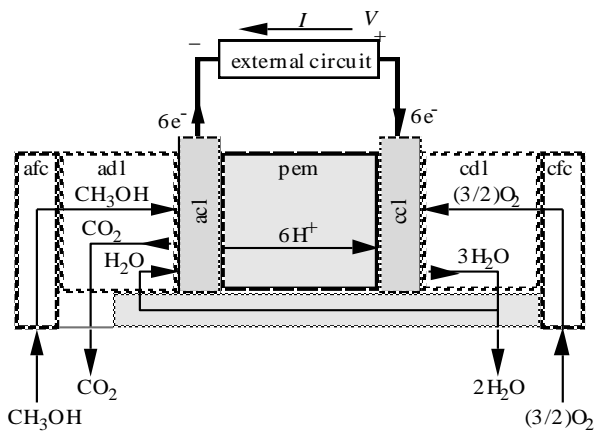


Fig. 2. DMFC schematic with reactant and particle flows (a=anode, c=cathode, pem=proton exchange membrane, fc= flow channel, dl=diffusion layer, cl=catalyst layer).

The methanol concentration  $C_{ah}$  along the anode flow channel depends on the methanol flow  $N_{ad}$  from the channel to the diffusion layer, as follows:

$$\delta_{ah} v_{ah} \frac{dC_{ah}}{dy} = -N_{ad} \quad (4)$$

On the other hand, this mass flow towards the diffusion layer can be determined as well by using the one-dimensional Fick's law:

$$N_{ad} = -D_{ad} \frac{dC_{ad}}{dx} \quad (5)$$

where  $D_{ad}$  is the methanol diffusivity in the anode diffusion layer.

It is worth noting that not all the methanol is oxidized at the anode catalyst layer, due to crossover through the membrane, i.e. some of the methanol permeates the membrane and reacts directly at the cathode without participating at the electric power generation. Thus, the overall methanol flow in (5) is given by the mass conservation law:

$$N_{ad} = \frac{J_a}{6F} + N_m \quad (6)$$

where  $J_a$  is the current density generated at the anode, i.e. the electron flow according to (2) and  $N_m$  is the methanol crossover flow. The parasitic flow of reactant through the membrane  $N_m$  can be calculated by adding the following terms, the first one related to diffusion, the other one related to electro-osmotic drag:

$$N_m = -D_m \frac{C_{ac}}{\delta_m} + n_d \frac{J_a}{F} \quad (7)$$

where  $C_{ac}$  is the methanol concentration at the CCL.

The current density at the anode in (6) is related to the activation voltage overpotential at the anode  $\eta_a$  by the Butler-Volmer equation [6], as

$$J_a = J_{a,ref} \left( \frac{C_{ac}}{C_{ac,ref}} \right)^{\gamma} \exp \left( \frac{\alpha_a F}{RT} \eta_a \right) \quad (8)$$

where  $J_{a,ref}$ ,  $C_{ac,ref}$  are the reference current density and the reference concentration at the anode, respectively. The voltage overpotential  $\eta_a$  is required to overcome the activation energy of the electrochemical reaction on the catalytic surface, and is associated to an energy loss.

The dependence between model parameters is fully non-linear, as it can be observed from the previous equations. Therefore, the anode current density can be expressed more conveniently as a function of the methanol concentration at the channel flow inlet  $C_{ah,in}$ , the crossover flow, and the overpotential as shown in [4], as:

$$J_a = \frac{J_{a,ref}}{C_{ac,ref}} \exp \left( \frac{\alpha_a F}{RT} \eta_a \right) \left[ \frac{\exp \xi_4 - 1}{\xi_4 (1 + \xi_3)} \left( C_{ah,in} + \frac{\delta_{ad} N_m}{D_{ad} \xi_3} \right) - \frac{1}{1 + \xi_3} \frac{\delta_{ad} N_m}{D_{ad} \xi_3} \right] \quad (8)$$

where  $\xi_3$ ,  $\xi_4$  are dimensionless parameters:

$$\xi_3 = \frac{1}{6F} \frac{\delta_{ad}}{D_{ad}} \frac{J_{a,ref}}{C_{ac,ref}} \exp \left( \frac{\alpha_a F}{RT} \eta_a \right) \quad (9)$$

$$\xi_4 = - \frac{l_{ah}}{\delta_{ah} v_{ah}} \frac{D_{ad}}{\delta_{ad}} \frac{\xi_3}{1 + \xi_3} \quad (10)$$

The anode current density  $J_a$  can be considered to be equal to the average current density  $J$  obtained as a ratio between the current flowing in the external circuit and the fuel cell cross-section. Resolving (7) in  $C_{ac}$  and substituting into (8), the following relationship between the current density and the activation overpotential at the anode (included in  $\xi_3$ ) is obtained:

$$J = \frac{\xi_3 (\exp \xi_4 - 1) D_m \delta_{ad} C_{ah,in}}{\xi_4 (1 + \xi_3) D_{ad} \delta_m} \frac{1}{\frac{1}{6F} - \frac{n_d}{F} \left[ \frac{\exp \xi_4 - 1}{\xi_4 \xi_5 (1 + \xi_3)} - \frac{1}{\xi_5} \right]} \quad (11)$$

where parameters  $\xi_3$ ,  $\xi_4$ ,  $\xi_5$  depend all on the activation overpotential  $\eta_a$ , and, in particular,  $\xi_5$  reads:

$$\xi_5 = 1 - \left[ \frac{\exp \xi_4 - 1}{\xi_3 \xi_4 (1 + \xi_3)} - \frac{1}{\xi_3} \right] \frac{D_m \delta_{ad}}{D_{ad} \delta_m} \quad (12)$$

It is worth noting that (11) is strongly non-linear, so that it should be inverted numerically in order to obtain the overpotential as a function of current density  $\eta_a = \eta_a(J)$ .

Relationships similar to (4)-(8) can be written for the cathode side, where the atmospheric oxygen is provided at catalyst layer through the gas diffusion layer and the flow channel. From these relations the current density can be derived, depending this time on the inlet oxygen concentration at cathode  $C_{ch,in}$ . It can be shown that the following approximated relation holds:

$$J = \frac{\frac{D_{cd}}{\delta_{cd}} C_{ch,in} - \frac{3 D_m \exp \xi_4 - 1}{2 \delta_m \xi_4 \xi_5 (1 + \xi_3)} C_{ah,in}}{\frac{1}{4F} \frac{1 + \xi_1}{\xi_1} + \frac{3 n_d}{2F \xi_5}} \quad (13)$$

where:

$$\xi_1 = \frac{1}{4F} \frac{\delta_{cd} J_{c,ref}}{D_{cd} C_{c,ref}} \exp\left(\frac{\alpha_c F}{RT} \eta_c\right) \quad (14)$$

is a dimensionless parameter related to the cathode. At this stage, the cathode overpotential can be obtained by inverting (13) as  $\eta_c = \eta_c(J)$  and it can be computed by using current and overvoltage values obtained from (11).

The reaction kinetic depends on temperature, according to (8). Consequently, the fuel cell system is described more accurately by a fully non-linear coupled model. Temperatures at the anode and cathode catalyst layers depend on the heat generation inside the DMFC, which is localized mainly at both catalyst layers. Keeping the cathode flow channel at room temperature, the heat flow is directed from the anode to the cathode along the x-axis, whereas the heat flux along the y-axis can be neglected without losing accuracy.

Heat generation is mainly due to reaction energies and water vapour condensation (at the cathode only). As shown in [5], the specific heat generation at the anode can be expressed as

$$q_{ac} = \eta_a i - \frac{H_a - G_a}{6F} i \quad (15)$$

where  $H_a$ ,  $G_a$  are the enthalpy and the Gibbs' free energy at the anode. These values are computed from the enthalpies of formation and from Gibbs' free energies of single reactants, according to [7].

In the same manner, the heat generation at the cathode can be computed as follows:

$$q_{cc} = \eta_c i - \frac{H_c - G_c}{6F} i - h_v N_{H_2O} \quad (16)$$

where  $h_v$  is the latent evaporation heat for water, and  $N_{H_2O}$  is the water vapour molar flow. Ohmic losses, due to the electric resistance of layers and collectors, can be neglected, due to small electric current density values. So the total heat generation can be computed from (15) and (16) as  $q_{tot} = q_{ac} + q_{cc}$ . The heat generated is entirely transferred to the external ambient by condensation and air exchange.

By using Newton's cooling law, the temperature at the cathode catalyst layer  $T_{cc}$  can be obtained, as:

$$q_{tot} = \frac{T_{cc} - T_r}{\frac{\delta_{cc}}{2\lambda_{cc}} + \frac{\delta_{cd}}{\lambda_{cd}}} \quad (17)$$

where  $T_r$  is the room temperature, and  $\lambda_{cc}$ ,  $\lambda_{cd}$  are the thermal conductivities of CCL and GDL.

Finally, the cell voltage at the current collectors as function of the current density can be computed from the previous anode and cathode overpotentials, as:

$$V(J) = E_o + \frac{\partial E}{\partial T} \Delta T - \eta_a(J) - \eta_c(J) - \frac{\delta_m}{\sigma_m} J - R_s J \quad (18)$$

where  $E_o$  is the (constant) standard cell potential,  $\sigma_m$  is the electric conductivity of the membrane, and  $R_s$  is the overall contact resistance per unit cross-section (that is assumed to be constant, and accounts for all resistances between gas diffusion layers and current collectors).

### 3. Numerical Experiments

In the following, an example of application of the 2D analytical model for an active-feed DMFC is provided.

The values of the geometric and physical quantities used in simulations are reported below. Geometric dimensions of the model are reported in Table. 2, while physical and thermal constants are listed in Tables. 3 and 4.

TABLE II. – Geometric parameters of the DMFC.

Parameter	Symbol	Value
Thickness of anode channel	$\delta_{ah}$	0.002 m
Thickness of cathode channel	$\delta_{ch}$	0.002 m
Width of anode channel	$w_{ah}$	0.002 m
Width of cathode channel	$w_{ch}$	0.002 m
Length of anode channel	$L_{ah}$	0.03 m
Length of cathode channel	$L_{ch}$	0.03 m
Width of anode channel	$w_{ah}$	0.003 m
Width of cathode channel	$w_{ch}$	0.003 m
Number of anode channels	$N_{ah}$	10
Number of cathode channels	$N_{ch}$	10
Thickness of the ADL	$\delta_{ad}$	$3 \cdot 10^{-4}$ m
Thickness of the CDL	$\delta_{cd}$	$3 \cdot 10^{-4}$ m
Thickness of the ACL	$\delta_{ac}$	$5 \cdot 10^{-5}$ m
Thickness of the CCL	$\delta_{cc}$	$3 \cdot 10^{-5}$ m
Thickness of the membrane	$\delta_m$	$2.06 \cdot 10^{-4}$ m

TABLE III. – Chemical/electrical constants of the DMFC.

Parameter	Symbol	Value
Anode inlet flow rate	$m_{ah}$	$2 \cdot 10^{-6} / 60 \text{ m}^3 \text{ s}^{-1}$
Cathode inlet flow rate	$m_{ch}$	$800 \cdot 10^{-6} / 60 \text{ m}^3 \text{ s}^{-1}$
Fluid velocity at the anode	$v_{ah}$	$m_{ah} / (N_{ah} w_{ah} \delta_{ah})$
Fluid velocity at the cathode	$v_{ch}$	$m_{ch} / (N_{ch} w_{ch} \delta_{ch})$
Inlet oxygen concentration	$C_{ch,in}$	$0.21 \cdot p / (RT) \text{ mol m}^{-3}$
Reference exchange current density at the anode	$J_{a,ref}$	$1.1 \cdot 10^4 \cdot \delta_{ac} \text{ A m}^{-2}$
Reference exchange current density at the cathode	$J_{c,ref}$	$1.1 \cdot 10^4 \cdot \delta_{cc} \text{ A m}^{-2}$
Reference concentration at the anode	$C_{a,ref}$	$10^3 \text{ mol m}^{-3}$
Reference concentration at the cathode	$C_{c,ref}$	$p / (RT) \text{ mol m}^{-3}$
Electro-osmotic drag coefficient	$n_d$	$2.9 \cdot \exp\left(\frac{1029}{333} - \frac{1029}{T}\right)$
Conductivity of the membrane	$\sigma_m$	$7.3 \cdot \exp\left(\frac{1268}{298} - \frac{1268}{T}\right)$
Ideal electromotive force in standard conditions	$E_o$	1.213 V
Rate of change of the electromotive force with the temperature	$\frac{\partial E}{\partial T}$	$-1.4 \cdot 10^4 \text{ V/K}$
Contact resistance	$R_s$	$8 \cdot 10^{-5} \Omega \text{ m}^2$

Diffusion coefficient of the methanol in the membrane	$D_m$	$4.9 \cdot 10^{-10} \exp\left(\frac{2436}{333} - \frac{2436}{T}\right)$ $m^2 s^{-1}$
Diffusion coefficient of the methanol in the ADL	$D_{ad}$	$1.54 \cdot 10^{-9} \exp\left(\frac{2436}{353} - \frac{2436}{T}\right)$ $m^2 s^{-1}$
Diffusion coefficient of the oxygen in the CCL	$D_{cd}$	$10^{-7} m^2 s^{-1}$
Anode transfer coefficient	$\alpha_a$	0.8
Cathode transfer coefficient	$\alpha_c$	0.8
Reaction order	$\gamma$	1
Ambient temperature	$T_r$	297.15 K
Air pressure at cathode inlet	$P$	$2.5 \cdot 1.01325 \cdot 10^5 Pa$

TABLE IV. – Thermal constants of the DMFC.

Parameter	Symbol	Value
Liquid methanol enthalpy of formation	$H_{MeOH}$	$-238.66 \cdot 10^3 J mol^{-1}$
Liquid water enthalpy of formation	$H_{H_2O}$	$-285.83 \cdot 10^3 J mol^{-1}$
Carbon dioxide enthalpy of formation	$H_{CO_2}$	$-393.51 \cdot 10^3 J mol^{-1}$
Liquid methanol Gibbs free energy	$G_{MeOH}$	$-166.27 \cdot 10^3 J mol^{-1}$
Liquid water Gibbs free energy	$G_{H_2O}$	$-237.08 \cdot 10^3 J mol^{-1}$
Carbon dioxide Gibbs free energy	$G_{CO_2}$	$-394.00 \cdot 10^3 J mol^{-1}$
Latent evaporation heat for water	$h_v$	$44.8610^3 J mol^{-1}$
Thermal conductivity of the membrane	$\lambda_m$	$0.21 W m^{-1} K^{-1}$
Thermal conductivity of the cathode diffusion layer	$\lambda_{cd}$	$1.6 W m^{-1} K^{-1}$
Liquid methanol specific heat capacity (at constant pressure)	$cp_{MeOH}$	$80.96 J mol^{-1} K^{-1}$
Liquid water specific heat capacity (at constant pressure)	$cp_{H_2O}$	$75.24 J mol^{-1} K^{-1}$
Carbon dioxide specific heat capacity (at constant pressure)	$cp_{CO_2}$	$36.9 J mol^{-1} K^{-1}$
Oxygen specific heat capacity (at constant pressure)	$cp_{O_2}$	$39.44 J mol^{-1} K^{-1}$

The proposed model is validated on experimental data provided in [8] for an active DMFC, maintained at a constant temperature of 90°C. Fig. 3 shows the polarization curves, obtained for various anode inlet methanol concentrations varying from 0.125 M to 0.625 M. It can be observed that numerically computed data are in good agreement with the experimental ones.

Numerical investigations show that average temperatures on the cross section are almost uniform across the DMFC layers (Fig. 4). This behaviour can be explained by noting that layers are very thin if compared to the cross section dimensions; however, the operating temperature strongly affects the electrical performance of the fuel cell as it can be noticed in Fig. 5.

Fig. 6 shows that the current density and, thus, the mass transport, depend more on cathode overpotential and less on the anode overpotential for high values of the anode inlet methanol concentration (0.625 M).

It can be shown that reactant concentrations vary along the y-axis almost linearly. The concentration, however, slightly depends on the layer width, much more on the current density. For example, Fig. 7 shows the methanol concentration computed on the anode catalyst layer.

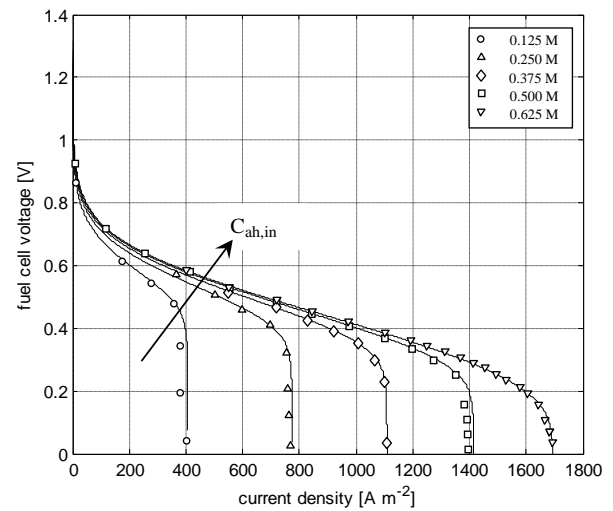


Fig. 3. Polarisation curves  $v-i$  for different methanol concentrations at the anode inlet (experimental values provided in [8] are compared with the computed ones).

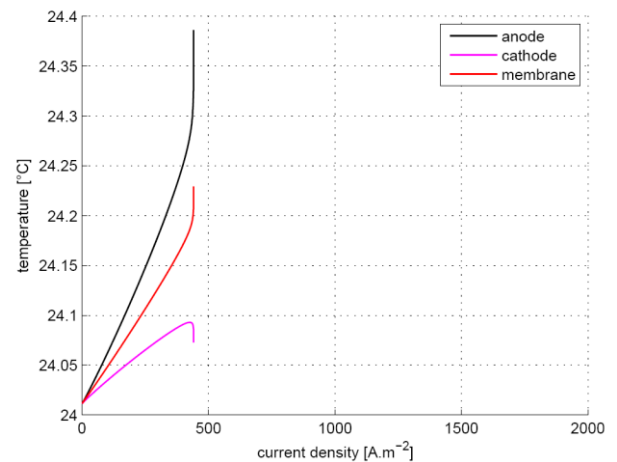


Fig. 4. Average temperatures on the membrane and on the catalyst layers (the room is temperature is 25°C, the anode inlet methanol concentration is 0.625 M).

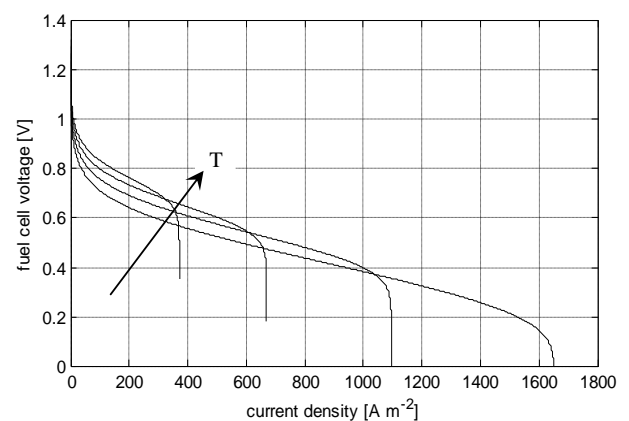


Fig. 5. Polarisation curves  $v-i$  for increasing average temperatures of DMFC ( $T=25,50,75,100^\circ C$ ); methanol concentration at the anode inlet is constant (0.5 M).

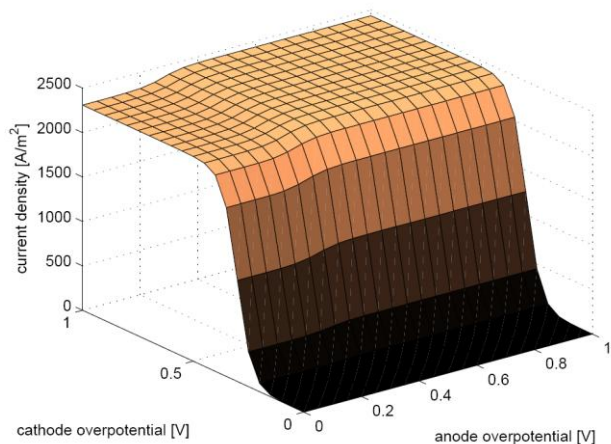


Fig. 6. Average current density vs. anode and cathode overpotentials (the anode inlet methanol concentration is constant 0.625 M,  $T=25^{\circ}\text{C}$ ).

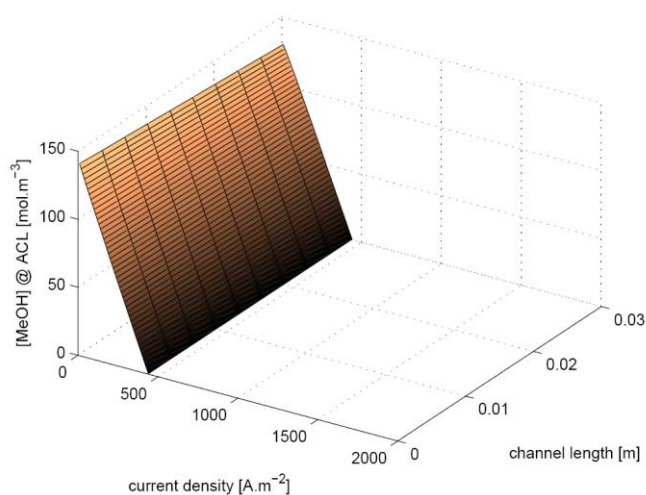


Fig. 7. Methanol concentration at the anode catalyst layer vs. current density and channel length (the anode inlet methanol concentration is 0.625 M,  $T=25^{\circ}\text{C}$ ).

#### 4. Conclusion

A two-dimensional model for analyse active-feed direct methanol fuel cells has been proposed. Electrochemical reactions at the anode and cathode electrodes, methanol

crossover, fluid flow in channels, reactant mass transport in diffusion layers and heat transfer effects are taken into account. An analytical solution of the model has been derived and numerically computed, in order to provide explicitly the relationship occurring between electric, thermal and chemical variables.

As a result, the model can be used for predicting the optimal design parameters of DMFC fuel cells under development at Padova University that make use of innovative materials for both catalyst layers and PEMs.

#### References

- [1] J. Larminie, A. Dicks, Fuel Cell Systems Explained, Wiley, Chichester (UK) (2003).
- [2] V. Di Noto, M. Piga, L. Piga, S. Polizzi and E. Negro, "New inorganic-organic proton conducting membranes based on Nafion<sup>®</sup> and  $[(\text{ZrO}_2)(\text{SiO}_2)_{0.67}]$  nanoparticles: Synthesis, vibrational studies and conductivity," to be published in *Journal of Power Sources*.
- [3] V. Di Noto, E. Negro, M. Piga, L. Piga, S. Lavina, G. Pace, "New Platinum-free Carbon Nitride Electrocatalysts for PEMFCs prepared using as precursors PAN/M(CNCH<sub>3</sub>)<sub>x</sub> complexes (M=Pd, Co, Au, Ni)," *ECS Trans.*, vol. 11, p. 249, 2007.
- [4] H. Guo and C.-F. Ma, "2D analytical model of a direct methanol fuel cell," *Electrochemistry Communications*, Vol. 6, pp. 306-312, 2004.
- [5] R. Chen and T. S. Zhao, "Mathematical modelling of a passive-feed DMFC with heat transfer effect," *Journal of Power Sources*, Vol. 152, pp. 122-130, 2005.
- [6] A. J. Bard, L. R. Faulkner, *Electrochemical Methods: Fundamentals and Applications*, Wiley, New York (2001).
- [7] P. Argyropoulos, K. Scott, W. M. Taama, "One-dimensional thermal model for direct methanol fuel cell stacks. Part 1: model development", *Journal of Power Sources*, Vol. 79, pp.169-183, 1999.
- [8] K. Scott, W. M. Taama, S. Kramer, P. Argyropoulos, K. Sundmacher, "Limiting current behaviour of the direct methanol fuel cell", *Electrochemical Acta*, Vol. 45, pp. 945-957, 1999.